

# EDGE/STRUCTURE PRESERVING SMOOTHING VIA RELATIVITY-OF-GAUSSIAN

Bolun Cai, Xiaofen Xing\*, Xiangmin Xu

South China University of Technology, Guangzhou, China  
caibolun@gmail.com, {xfxing, xmxu}@scut.edu.cn

## ABSTRACT

This paper presents a novel edge/structure-preserving image smoothing via relativity-of-Gaussian. As a simple local regularization, it performs the local analysis of scale features and globally optimizes its results into a piecewise smooth. The central idea to ensure proper texture smoothing is based on cross-scale relative that captures the weak textures from the most prominent edges/structures. Our method outperforms the previous methods in removing the detail information while preserving main image content.

**Index Terms**— Image smoothing, edge/structure preserving, relative-of-Gaussian

## 1. INTRODUCTION

Edge/structure-preserving image smoothing has recently emerged as a valuable tool for a variety of applications in image processing. In particular, it is often used to decompose an image into a piecewise-smooth base layer and a local-volatile detail layer. Such a decomposition may then be used for detail enhancement [1, 2], HDR tone mapping [3, 4], structure extraction [5, 6], and for other tasks.

Depending on the application, the preserving image smoothing operators (in Fig. 1) may be manipulated separately in various ways, which can be divided into *local filter* and *global optimization*.

- **Local filter** is developed in different strategies, including bilateral filter (BLF) [7] and local extrema filter (LEF) [8]. These edge-aware filters tradeoff between details flattening and edge preservation between neighboring pixels by considering intensity difference. However, Gibbs phenomenon of local filters will result in ringing-effect on the edge.

- **Global optimization** methods include total variation (TV) [9], weighted least squares (WLS) [1] and relative total variation (RTV) [5]. These methods restore images by global optimization functions containing terms defined in L1 norm, weighted L2 norm or relative norm. However, they all fo-

cus on relatively small variance suppression and vulnerable to textures.

We address these problems by proposing an edge/structure-preserving image smoothing that can remove the texture at any level. A *local regularization* called Relativity-of-Gaussian (RoG) is *optimized globally* to identify potential edges at any scale. As demonstrated in Fig.1 (g), the proposed method can effectively eliminate texture without distorting edge/structure.

## 2. SMOOTHING VIA RELATIVITY-OF-GAUSSIAN

### 2.1. Local Regularization

To identify variance at different scales, the Gaussian kernel and its derivatives [10, 11, 12] are the effective smoothing kernels for scale analysis. Such as [13], Difference-of-Gaussian (DoG) was applied to locate key-points and identify scales of high variation. Inspired by DoG, we describe a local regularization called Relativity-of-Gaussian (RoG) to selectively smooth the gradient  $\nabla S$ . The RoG regularization is finally expressed as

$$\mathcal{R} = \left| \frac{G_{\sigma_1} * \nabla S}{G_{\sigma_2} * \nabla S} \right|, \text{s.t. } \sigma_1 < \sigma_2. \quad (1)$$

A local Gaussian kernel  $G_\sigma$  is defined for scale selection:  $G_\sigma(x, y) = \exp\left(-\frac{1}{2\sigma}\left((x - x_0)^2 + (y - y_0)^2\right)\right)$ , where  $\sigma$  is a scale parameter and  $(x_0, y_0)$  is the center of the kernel.

We show a synthetic patch in Fig. 1 (a) contains weak textures and strong edges/structures. Shown in Fig. 2, the small-scale feature  $|G_{\sigma_1} * \nabla S|$  contains almost all gradients as (a); the large-scale feature  $|G_{\sigma_2} * \nabla S|$  only contains strong edges/structures as (b); the cross-scale relative is equivalent to DoG to identify the variances at one scale as (c). Another intuitive explanation of RoG is that a strong edge/structure with identical patterns in neighbor contributes more similar-direction gradients than weak texture with complex patterns.

### 2.2. Global Optimization

To effectively smooth different scale edges of the input image  $I$ , the global optimization function is finally expressed by

\* X. Xing is the corresponding author. This work is supported by National Natural Science Founding of China (61171142, 61401163, U1636218), Fundamental Research Funds for Central Universities (2017MS045), Guangzhou Key Lab of Body Data Science (201605030011), and Science and Technology Planning Project of Guangdong (2014B010111003, 2014B010111006).

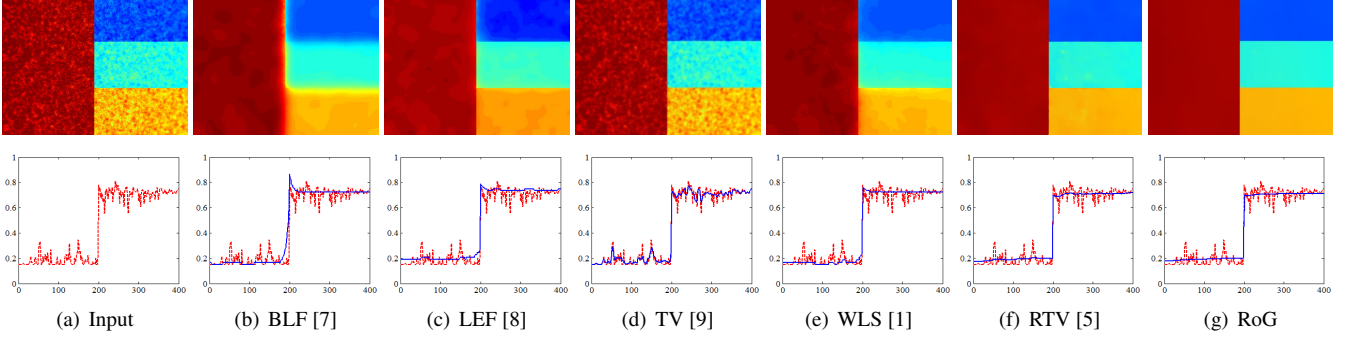


**Fig. 1.** Compare different edge/structure-preserving image smoothing on a noisy image. (a) Input. (b) BLF ( $\sigma_s = 12$ ,  $\sigma_r = 0.45$ ). (c) LEF ( $r = 3$ ). (d) TV ( $\theta = 30$ ). (e) WLS ( $\lambda = 0.35$ ,  $\alpha = 1.8$ ). (f) RTV ( $\lambda = 0.015$ ,  $\sigma = 3$ ). (g) RoG ( $K = 3$ ,  $\lambda = 0.01$ ,  $\sigma_1 = 1$ ,  $\sigma_2 = 3$ ).

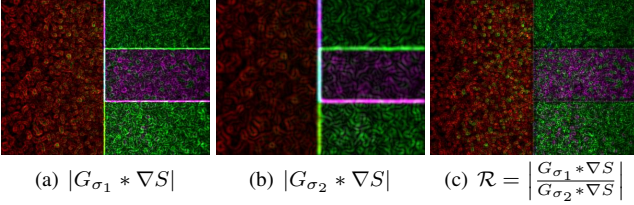


**Fig. 2.** RoG regularization captures the textures from the prominent edges/structures (small-scale:  $\sigma_1 = 1$ , large-scale:  $\sigma_2 = 3$ ).

taking the RoG regularization:

$$\arg \min_S \|S - I\|_2^2 + \lambda \left( \left\| \frac{G_{\sigma_1} * \nabla_x S}{G_{\sigma_2} * \nabla_x S} \right\|_1 + \left\| \frac{G_{\sigma_1} * \nabla_y S}{G_{\sigma_2} * \nabla_y S} \right\|_1 \right), \quad (2)$$

where  $I$  is the intensity of luminance or color channels, and  $\lambda$  is the positive parameter. The first term  $\|S - I\|_2^2$ , which corresponds to L2 data fidelity, is to minimize the distance between smoothing result  $S$  and the input image  $I$ .

Since the RoG regularization is an L1-norm, its solution cannot be obtained trivially. An iteratively re-weighted least square [14] method is introduced to solve non-convex regularization. The x-direction RoG regularization is discussed, and the y-direction term can be dealt with similarly. By re-organizing the regularization, x-direction RoG is written as:

$$\begin{aligned} \left\| \frac{G_{\sigma_1} * \nabla_x S}{G_{\sigma_2} * \nabla_x S} \right\|_1 &= \left\| \frac{(G_{\sigma_1} * \nabla_x S)^2}{(G_{\sigma_2} * \nabla_x S)(G_{\sigma_1} * \nabla_x S)} \right\|_1 \\ &\approx \left\| \frac{G_{\sigma_1/2} * (\nabla_x S)^2}{(G_{\sigma_2} * \nabla_x S)(G_{\sigma_1} * \nabla_x S)} \right\|_1 \\ &= G_{\sigma_1/2} * \frac{1}{|(G_{\sigma_2} * \nabla_x S)(G_{\sigma_1} * \nabla_x S)|} \|\nabla_x S\|_2^2 \end{aligned} \quad (3)$$

The second line in (3) is an approximation due to the convolution decomposition for numerical solution. Then the RoG regularization is decomposed into a quadratic term  $\|\nabla_x S\|_2^2$

and a non-linear weight  $w_{x,y}$  as

$$w_{x,y} = G_{\sigma_1/2} * \frac{1}{|(G_{\sigma_2} * \nabla_{x,y} S)(G_{\sigma_1} * \nabla_{x,y} S)|} \quad (4)$$

Therefore, the global optimization is iteratively cycled through. In particular, for the  $k$ -th iteration:

$$S^k = \arg \min_S \|S - I\|_2^2 + \lambda \left( w_x \|\nabla_x S^{k-1}\|_2^2 + w_y \|\nabla_y S^{k-1}\|_2^2 \right) \quad (5)$$

Initializing  $S^0 = I$ , we use matrix notation to rewrite the loss function following quadratic form:

$$(\mathbf{S} - \mathbf{I})^T (\mathbf{S} - \mathbf{I}) + \lambda (\mathbf{S}^T \mathbf{D}_x^T \mathbf{W}_x \mathbf{D}_x \mathbf{S} + \mathbf{S}^T \mathbf{D}_y^T \mathbf{W}_y \mathbf{D}_y \mathbf{S}). \quad (6)$$

Here  $\mathbf{S}$  and  $\mathbf{I}$  are the vector representation of  $S$  and  $I$  respectively,  $\mathbf{W}_{x,y}$  is diagonal matrices containing the weights  $w_{x,y}$ , and the matrices  $\mathbf{D}_x$  and  $\mathbf{D}_y$  are discrete differentiation operators. The vector  $\mathbf{S}$  that minimizes Eq.(6) is uniquely defined as the solution of a linear system

$$\mathbf{S}^k = (\mathbf{1} + \lambda \mathbf{L}^{k-1})^{-1} \mathbf{I}. \quad (7)$$

Here  $\mathbf{1}$  is an identity matrix and  $\mathbf{L}^k = \mathbf{D}_x^T \mathbf{W}_x^k \mathbf{D}_x + \mathbf{D}_y^T \mathbf{W}_y^k \mathbf{D}_y$  is a sparse five-point Laplacian matrix [15]. To reach  $O(N)$  complexity, a fast solver called preconditioned conjugate gradient (PCG) [16] is used for speedup. The whole optimization process is summarized in Algorithm 1.

### 2.3. Analysis

We analyze the RoG regularization with a few others on p-preserving image smoothing, including edge-preserving and structure-preserving.

#### 2.3.1. Edge-preserving Smoothing

In Algorithm 1, if the maximum iterations number  $K = 1$ , the object function is similarly turned to WLS [1], an edge-preserving method. Differently to WLS, RoG calculates the

**Algorithm 1** Edge/Structure Preserving Smoothing via RoG

**Input:** Input image  $\mathbf{I}$ , scale parameter  $\sigma_{1,2}$ , positive parameter  $\lambda$  and maximum iterations  $K$ .

**Output:** Smoothing result  $\mathbf{S}$ .

- 1: initialize  $\mathbf{S}^0 \leftarrow \mathbf{I}$
- 2: **for**  $k = 1$  to  $K$  **do**
- 3:   compute weights  $w_{x,y}$  in Eq. (4)
- 4:   update  $\mathbf{S}^k$  using (7)
- 5: **end for**

weights by original signal without the logarithmic transform. While the logarithmic transform simulates human vision perception mechanism described by Weber's law [17]. Given a stimulus signal  $S$ , the WLS's weight in the log-transformed domain is  $(\nabla \log S)^{-1} = S/\nabla S$ . When  $S$  is very large,  $(\nabla \log S)^{-1}$  is amplified by  $S$ , which inevitably dominates over the smoothing term in the high magnitude areas as Fig. 3 (b). Therefore, RoG uses the relative function on original signal to preserve the edges coequally in the high and low magnitude areas as Fig. 3 (c).

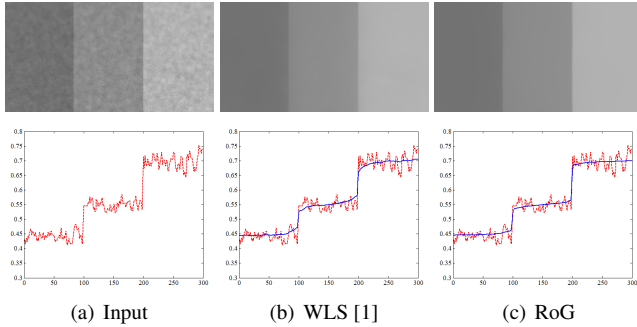


**Fig. 3.** Compare edge-preserving scheme with WLS. (b) WL-S ( $\lambda = 1.0$ ,  $\alpha = 1.2$ ). The second edge in the high magnitude areas is smoothed more than the first. (c) RoG ( $K = 1$ , the others are same as Fig.1).

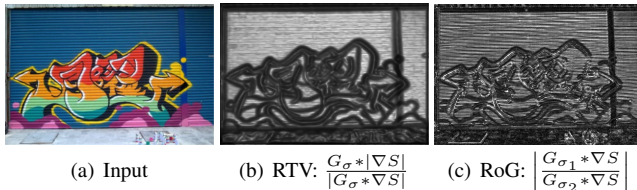


**Fig. 4.** Compare structure-preserving scheme with RTV. (b) RTV:  $\frac{G_\sigma * |\nabla S|}{|G_\sigma * \nabla S|}$ . (c) RoG:  $\left| \frac{G_{\sigma_1} * \nabla S}{G_{\sigma_2} * \nabla S} \right|$ . RoG regularization captures more clear textures without prominent structures.

### 2.3.2. Structure-preserving Smoothing

When  $K > 1$ , the proposed solver is similarity to an iterative method for RTV [5] to extract structure from texture. For

RTV, structure feature is computed in a patch centered with a single-scale Gaussian kernel, in which case the patches for two adjacent pixels should have a large overlap, reducing the feature discriminability. In contrast, RoG calculates the relative function with different Gaussian kernels ( $\sigma_1 < \sigma_2$ ) to stay clear of a prominent structure with high-resolution as Fig. 4 (c). Moreover, the relativity of cross-scale is a kind of band-passed filter to selectively extract structures at any level.

## 3. EXPERIMENTS

To verify the edge/structure-preserving image smoothing, a number of effective tools are implemented with RoG regularization for detail enhancement, HDR tone mapping, and structure extraction. We briefly describe these tools <sup>1</sup> and show the comparison results with state-of-the-art methods.

### 3.1. Detail Enhancement

As a nonlinear edge-preserving image smoothing ( $K = 1$ ), our method can be used for detail enhancement via base and detail layer decomposition. For example, we can simply replace the edge-preserving smoothing in the classical detail enhancement framework with RoG-based smoothing. Halo artifact and noise amplification are two major problems to be addressed for detail enhancement. RoG-based detail enhancement avoid the mild halo and noise that are sometimes visible in state-of-the-art results (in Fig. 5). To enhance the details at multi-scale shown in Fig. 6, we also can construct a multi-scale decomposition via  $\sigma_{1,2}$ , which controls the exposure and contrast of the base layer.



(a) Coarse-scale boost    (b) Fine-scale boost    (c) Combine

**Fig. 6.** Multi-scale detail enhancement with RoG edge-preserving smoothing. ( $K = 1$ ,  $\lambda = 0.001$ , coarse-scale:  $\sigma_1 = 1.0$  and  $\sigma_2 = 1.5$ , fine-scale:  $\sigma_1 = 0.5$  and  $\sigma_2 = 1.0$ )

### 3.2. HDR Tone Mapping

One of the challenges in image processing is the rendering of a High-Dynamic Range (HDR) scene on a conventional Low-Dynamic Range (LDR) display. RoG smoothing is also easily harnessed to perform tone mapping of HDR images. Based on [3], the LCIS-based decomposition is simply replaced by our RoG-based smoothing. Since multi-exposure fusion is the major problem to display surface reflections for

<sup>1</sup>More tools and comparisons can be found at <https://caibolun.github.io/RoG/>.

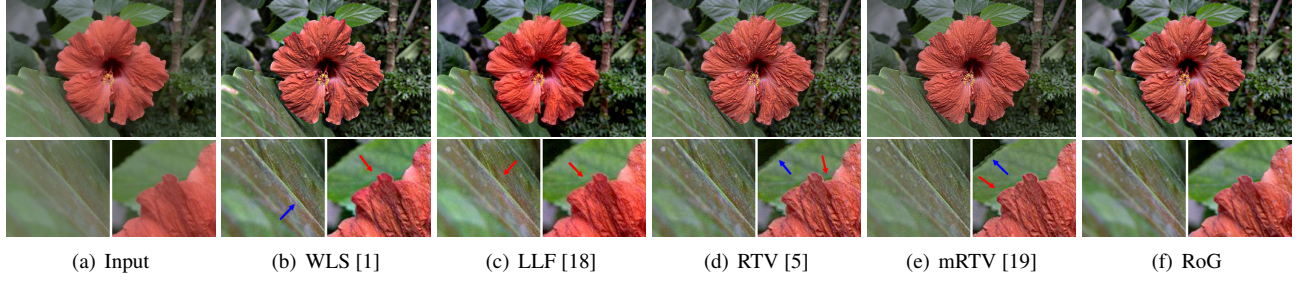


**Fig. 5.** Detail enhancement compared with previous methods. *In the close-ups, blue arrows point to the halo artifacts, and red arrows point to the noise amplifications.* (b) WLS ( $\lambda = 1.0$ ,  $\alpha = 1.2$ ). (c) LLF ( $\alpha = 2$ ,  $\sigma_r = 0.4$ ). (d) RTV ( $\lambda = 0.015$ ,  $\sigma = 0.5$ ). (e) mRTV ( $k = 3$ ,  $n_{itr} = 5$ ). (f) RoG ( $K = 1$ ,  $\lambda = 0.001$ ,  $\sigma_1 = 0.5$ ,  $\sigma_2 = 1.0$ ).

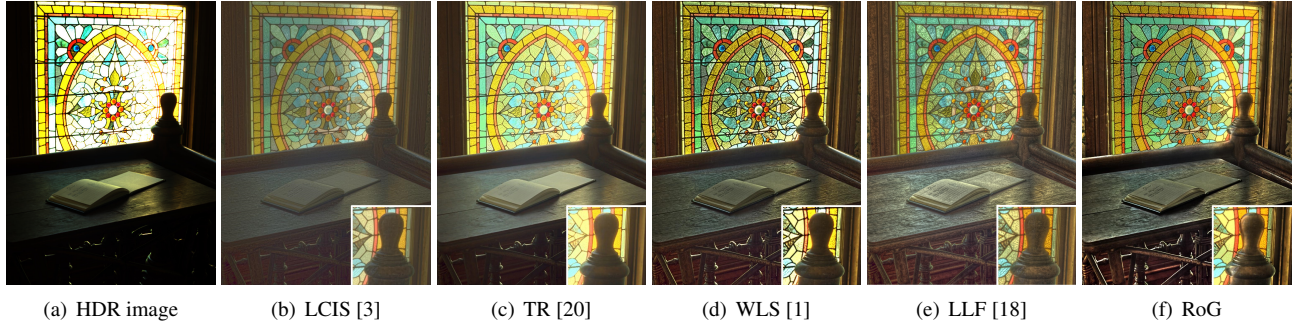


**Fig. 7.** HDR tone mapping compared with previous methods. *The wood gloss is only restored faultlessly by RoG-based method.*

HDR tone mapping, an exact base-layer decomposition is the key to produce a LDR image. In Fig. 7, the gloss is hard to be restored with high-level sheen except to RoG.

### 3.3. Structure Extraction

We compare our method with the state-of-the-art image smoothing techniques that were specifically designed for structure-texture separation. The main structures are formed by many edge with salient but fine texture boundaries, making structure extraction very challenging. An excellent structure extraction can capture really structures and reduce texture interference. Results from RoG and other methods are presented in Fig. 8, and we have hand tuned parameters for these methods.

## 4. CONCLUSION

We have presented an image smoothing methods via a novel regularization called RoG, which is effectively to remove textures while preserving other content. The RoG regularization is greatly extensible to accommodate various tools, and yields decent performance. RoG is a general concept and does not depend on any specific definition of scale feature. Therefore, our future work will be to apply it to more applications.

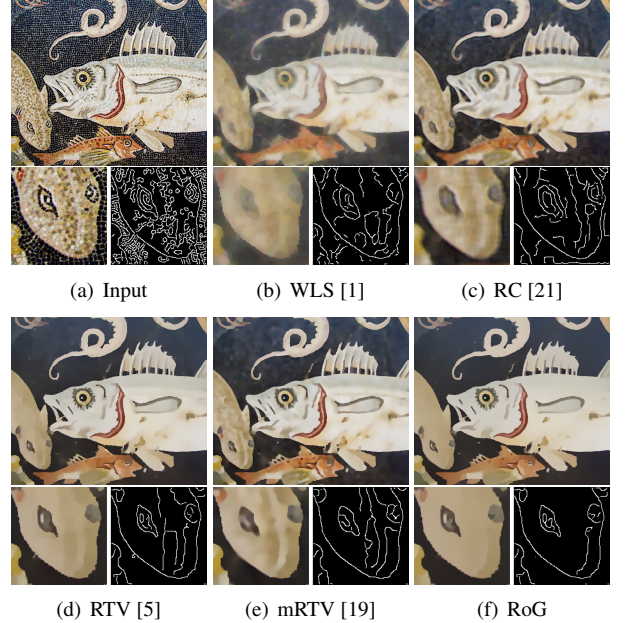


**Fig. 8.** Structure-preserving smoothing results, close-ups and structure maps (generated by Canny [22]) compared with previous methods. *The result based on RoG is smooth on the fish-scales with the preserving of the fish eye.* (b) WLS ( $\lambda = 1.0$ ,  $\alpha = 1.2$ ,  $k = 13$ ). (c) RC ( $\sigma = 0.2$ ,  $k = 19$ , Mod I). (d) RTV ( $\lambda = 0.015$ ,  $\sigma = 6$ ). (e) mRTV ( $k = 7$ ,  $n_{itr} = 5$ ). (f) RoG ( $K = 4$ ,  $\lambda = 0.01$ ,  $\sigma_1 = 2$ ,  $\sigma_2 = 4$ ).

## 5. REFERENCES

- [1] Zeev Farbman, Raanan Fattal, Dani Lischinski, and Richard Szeliski, “Edge-preserving decompositions for multi-scale tone and detail manipulation,” in *ACM Transactions on Graphics (TOG)*. ACM, 2008, vol. 27, p. 67.
- [2] Pietro Perona and Jitendra Malik, “Scale-space and edge detection using anisotropic diffusion,” *IEEE Transactions on pattern analysis and machine intelligence*, vol. 12, no. 7, pp. 629–639, 1990.
- [3] Jack Tumblin and Greg Turk, “LCIS: A boundary hierarchy for detail-preserving contrast reduction,” in *Proceedings of the 26th annual conference on Computer graphics and interactive techniques*. ACM Press/Addison-Wesley Publishing Co., 1999, pp. 83–90.
- [4] Zhengguo Li, Jinghong Zheng, Zijian Zhu, Wei Yao, and Shiqian Wu, “Weighted guided image filtering,” *IEEE Transactions on Image Processing*, vol. 24, no. 1, pp. 120–129, 2015.
- [5] Li Xu, Qiong Yan, Yang Xia, and Jiaya Jia, “Structure extraction from texture via relative total variation,” *ACM Transactions on Graphics (TOG)*, vol. 31, no. 6, pp. 139, 2012.
- [6] Yijun Li, Jia-Bin Huang, Narendra Ahuja, and Ming-Hsuan Yang, “Deep joint image filtering,” in *European Conference on Computer Vision*. Springer, 2016, pp. 154–169.
- [7] Carlo Tomasi and Roberto Manduchi, “Bilateral filtering for gray and color images,” in *Computer Vision, 1998. Sixth International Conference on*. IEEE, 1998, pp. 839–846.
- [8] Kartic Subr, Cyril Soler, and Frédéric Durand, “Edge-preserving multiscale image decomposition based on local extrema,” *ACM Transactions on Graphics (TOG)*, vol. 28, no. 5, pp. 147, 2009.
- [9] Leonid I Rudin, Stanley Osher, and Emad Fatemi, “Nonlinear total variation based noise removal algorithms,” *Physica D: Nonlinear Phenomena*, vol. 60, no. 1-4, pp. 259–268, 1992.
- [10] David G Lowe, “Object recognition from local scale-invariant features,” in *Computer vision, 1999. The proceedings of the seventh IEEE international conference on*. Ieee, 1999, vol. 2, pp. 1150–1157.
- [11] Tony Lindeberg, “Scale-space theory: A basic tool for analyzing structures at different scales,” *Journal of applied statistics*, vol. 21, no. 1-2, pp. 225–270, 1994.
- [12] Krystian Mikolajczyk and Cordelia Schmid, “An affine invariant interest point detector,” in *European conference on computer vision*. Springer, 2002, pp. 128–142.
- [13] David G Lowe, “Distinctive image features from scale-invariant keypoints,” *International journal of computer vision*, vol. 60, no. 2, pp. 91–110, 2004.
- [14] Emmanuel J Candes, Michael B Wakin, and Stephen P Boyd, “Enhancing sparsity by reweighted  $\ell_1$  minimization,” *Journal of Fourier analysis and applications*, vol. 14, no. 5-6, pp. 877–905, 2008.
- [15] Dilip Krishnan, Raanan Fattal, and Richard Szeliski, “Efficient preconditioning of laplacian matrices for computer graphics,” *ACM Transactions on Graphics (TOG)*, vol. 32, no. 4, pp. 142, 2013.
- [16] Richard Barrett, Michael Berry, Tony F Chan, James Demmel, June Donato, Jack Dongarra, Victor Eijkhout, Roldan Pozo, Charles Romine, and Henk Van der Vorst, *Templates for the solution of linear systems: building blocks for iterative methods*, SIAM, 1994.
- [17] William F Schreiber, *Fundamentals of electronic imaging systems: some aspects of image processing*, vol. 15, Springer Science & Business Media, 2012.
- [18] Sylvain Paris, Samuel W Hasinoff, and Jan Kautz, “Local Laplacian filters: Edge-aware image processing with a laplacian pyramid.,” *ACM Trans. Graph.*, vol. 30, no. 4, pp. 68, 2011.
- [19] Hojin Cho, Hyunjoon Lee, Henry Kang, and Seungyong Lee, “Bilateral texture filtering,” *ACM Transactions on Graphics (TOG)*, vol. 33, no. 4, pp. 128, 2014.
- [20] Erik Reinhard, Michael Stark, Peter Shirley, and James Ferwerda, “Photographic tone reproduction for digital images,” *ACM transactions on graphics (TOG)*, vol. 21, no. 3, pp. 267–276, 2002.
- [21] Levent Karacan, Erkut Erdem, and Aykut Erdem, “Structure-preserving image smoothing via region covariances,” *ACM Transactions on Graphics (TOG)*, vol. 32, no. 6, pp. 176, 2013.
- [22] John Canny, “A computational approach to edge detection,” *IEEE Transactions on pattern analysis and machine intelligence*, , no. 6, pp. 679–698, 1986.